

## Enhanced Generator Controls for the Improvement of Power System Voltage Stability

John J. Paserba<sup>1,\*</sup>, Masaru Shimomura<sup>2</sup>, Seiichi Tanaka<sup>2</sup>, Donald J. Shoup<sup>1</sup>, Robert T. Hellested<sup>1,\*\*</sup>

<sup>1</sup>Mitsubishi Electric Power Products, Inc., Warrendale, Pennsylvania, USA

<sup>2</sup>Mitsubishi Electric Corporation, Kobe, Japan

**Summary:** Voltage instability problems are attracting increasing attention in today's power systems, with wide-ranging emphasis on power system operation, planning, and control. This paper describes various means to improve power system voltage stability by enhancing generator reactive and active power control and voltage control, along with application examples. The areas discussed are High Side Voltage Control (HSVC), advanced Over-Excitation Limiters (OEL), and Adjustable Speed Machines (ASM).

**Keywords:** Secondary Voltage Control, Automatic Voltage Regulator, Excitation Systems, Voltage Stability, Over-Excitation Limiter, High Side Voltage Control, Adjustable Speed Machine

### 1. INTRODUCTION

Voltage instability problems are attracting increasing attention in today's power systems, with wide-ranging emphasis on power system operation, planning, and control [1, 2, 3]. These problems are becoming a more serious concern with the ever-increasing utilization and higher loading of existing transmission systems, particularly with increasing energy demands, and competitive generation and supply requirements. It is well established that enhancing the reactive power supplying ability of a power system by applying synchronous condensers, shunt and series capacitor banks, static compensators (STATCOM), static var compensators (SVCs), and other Flexible AC Transmission System (FACTS) controllers is effective in improving voltage stability. However, other possibilities are available for the improvement of voltage stability that can be applied on generators by enhancing their reactive and active power control and voltage control. For example, methods such as High Side Voltage Control (HSVC), advanced Over-Excitation Limiters (OEL), and the application of adjustable speed machines (ASM) have all been developed and applied for the improvement of voltage stability. This paper describes various ways to improve power system voltage stability by enhancing generator controls, including application examples.

### 2. HIGH SIDE VOLTAGE CONTROL

#### 2.1 Introduction

The advanced High Side Voltage Control (HSVC) regulator controls the high side voltage of a generator step-up transformer with no requirement for a direct feedback signal (i.e., measurement) from the high

voltage side.

The concept and implementation of the HSVC is an improvement over other methods of supplemental generator excitation control, such as the line drop compensator (LDC), which compensates the voltage drop by a reactive current, and the power system voltage regulator (PSVR), which uses a direct-measurement of the high side voltage as a feedback signal [4]. The advanced HSVC is superior to these methods with respect to control performance, reliability, and economics, as described in the following subsections.

#### 2.2 Principles and Characteristics of HSVC

The configuration of the advanced HSVC is shown in Figure 2-1. The basic function of the advanced HSVC for a simple power system, shown in Figure 2-2, is described in the following subsections.

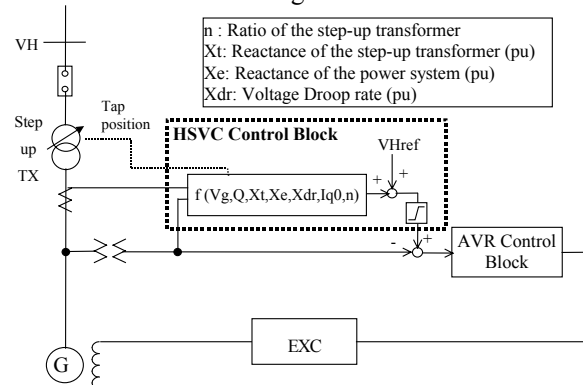


Figure 2-1. Configuration of HSVC control system

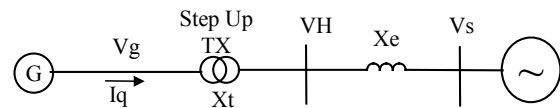


Figure 2-2. Simple power system

#### 2.2.1 Basic Function

With a target setting value of the high side voltage (VHref), the generator terminal voltage (Vg), i.e., the low side voltage, is controlled to be:

$$V_g = V_{Href} + (X_t - X_{dr}) I_q \quad (2-1)$$

Where,  $I_q = Q / V_g$ . The resultant high side voltage (VH) becomes:

$$V_H = V_{Href} - X_{dr} I_q \quad (2-2)$$

This characteristic can be expressed as shown in Figure 2-3.

\* 549B Keystone Drive, Warrendale, Pennsylvania, USA 15086: [j.paserba@ieee.org](mailto:j.paserba@ieee.org)

\*\* With acknowledgements to Yuou Xia, Hitomi Kitamura, Masaru Wakabayashi

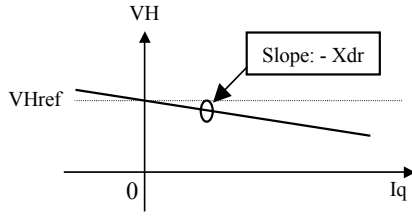


Figure 2-3. Characteristics of HSVC

For a target high side voltage reference ( $V_{Href}$ ), the high side voltage ( $V_H$ ) can be controlled to only drop for part of the voltage droop rate ( $X_{dr}$ ). This voltage droop rate ( $X_{dr}$ ) is necessary for stable parallel operation among multiple generators.

### 2.2.2 Reactive Current Compensation Function

To control the high side voltage ( $V_H$ ) to the reference value ( $V_{Href}$ ) at the specified reactive current ( $I_{q0}$ ), a supplemental control can be adopted by using  $I_{q0}$ . The high side voltage ( $V_H$ ) at large reactive current can be kept to a higher value by this function. The generator terminal voltage ( $V_g$ ) is controlled to be:

$$V_g = V_{Href} + X_t I_q - X_{dr} (I_q - I_{q0}) \quad (2-3)$$

and the high side voltage ( $V_H$ ) becomes:

$$V_H = V_{Href} - X_{dr} (I_q - I_{q0}) \quad (2-4)$$

This characteristics can be expressed as shown in Figure 2-4.

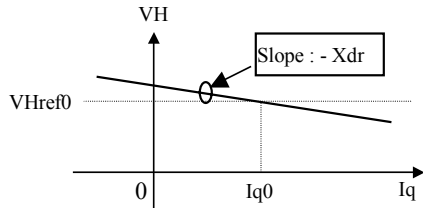


Figure 2-4. Characteristics of reactive current compensation function

### 2.2.3 Reactive Current Compensation Function by $X_e$

This function is used to follow the reactive current ( $I_{q0}$ ) automatically, corresponding to the variation of the reference voltage ( $V_{Href}$ ). For an original reference setting value ( $V_{Href0}$ ) and an external reactance ( $X_e$ ), a change of the reactive current ( $\Delta I_{q0}$ ) by a new setting value reference voltage ( $V_{Href}$ ) is approximately given by Equation (2-5).

$$\Delta I_{q0} = (V_{Href} - V_{Href0})/X_e \quad (2-5)$$

Therefore, this function can be realized by adding Equation (2-5) to the reactive current ( $I_{q0}$ ) in Equations (2-3) and (2-4).

### 2.2.4 Compensation Function of the Droop Rate Corresponding to the Variation of the Tap Position of the Step-Up Transformer

When the generator terminal voltage ( $V_g$ ) is controlled by the advanced HSVC, it may be generally maintained higher than its rated voltage in order to keep the high side voltage ( $V_H$ ) at a constant value. On the other hand, the continuous allowable generator terminal voltage ( $V_g$ ) is generally limited to 105% of its rated

voltage. If the generator terminal voltage ( $V_g$ ) is near this maximum voltage in a steady state operation, the improving effect of the voltage stability by the advanced HSVC is reduced by this limitation. Therefore, in the case of a step-up transformer with load-tap-changer (LTC), the coordinated control between the HSVC and the tap position control can increase the ability of the HSVC by keeping the generator terminal voltage ( $V_g$ ) to near its rated voltage in steady state condition. The separation of functions shown in Table 2-1 between the advanced HSVC and the LTC control functions is a suitable solution to improving the voltage stability.

Table 2-1. Primary Functions for HSVC and LTC Control

Control	Function
HSVC	Controls high side voltage ( $V_H$ ) to a reference value ( $V_{Href}$ )
LTC control	Controls generator terminal voltage ( $V_g$ ) to near the rated voltage

However, the droop rate changes according to the variation of the voltage ratio and the reactance of the step-up transformer ( $X_t$ ), depending on its tap position. As a result, the parallel operation among adjacent generators may become difficult due to an unbalance of reactive power on each generator, which is caused by the discrepancy of the tap positions of each step-up transformer. For preventing this condition, a compensation function that keeps the droop rate constant corresponding to the tap position, can be added to the HSVC. For the case where a change of the tap position causes a change of the voltage ratio and the reactance by the same ratio ( $n$ ), the basic control function is changed from Equation (2-1) to (2-6).

$$V_g = V_{Href} / n + (X_t - X_{dr}/n) I_q \quad (2-6)$$

Then, the resultant high side voltage ( $V_H$ ) becomes the same as Equation (2-2).

As mentioned above, although this specific characteristic is the same as with the application of line drop compensator (LDC), the advanced HSVC has the following superior features [5]:

- The high side reference voltage ( $V_{Href}$ ) can be directly set to a desired value from local and/or remote location. Accordingly, the coordinated control of the power system voltage among multiple generators and/or substations is possible.
- A feedback signal (i.e., measurement) of a high side voltage is not required.
- The following optional functions can be added to the HSVC:
  - Reactive current compensation function.
  - Reactive current compensation function by an external reactance.
  - Compensation function of the droop rate corresponding to the variation of the tap position of the step-up transformer.
- Additional optional features of the advanced HSVC discussed in detail in Reference [5] include:

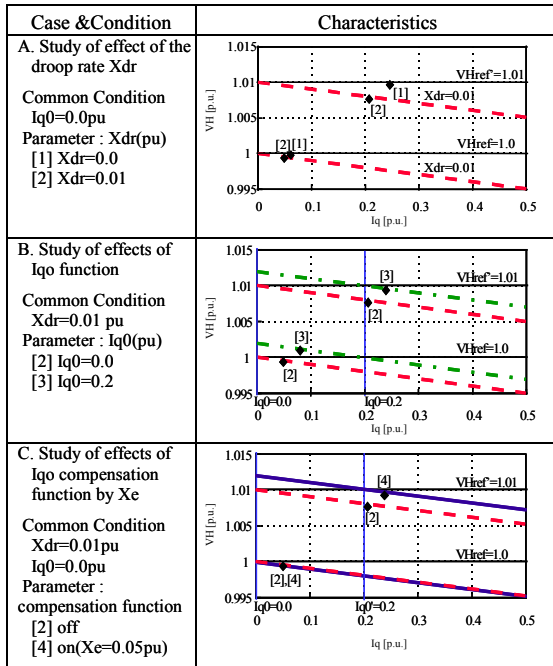
- A phase compensation function to further improve stability by modifying the response characteristics of the HSVC control loop.
- A phase compensation function for power swing damping to improve the oscillatory stability of a power system.

### 2.2.5 Verification of the HSVC Functions

The performance of the HSVC described in the equations presented in this subsection was verified by simulation analysis of a step-change of the high side voltage reference (VHref) from 1.0 p.u. to 1.01 p.u. on a simple power system. These results are shown in Figure 2-5 and Figure 2-6. Figure 2-5 shows each resultant characteristic, which is plotted according to the simulation results before and after a step-change. Each case shows the theoretical characteristics by the dashed or solid lines and the simulated results by the points.

Case A shows the droop characteristics of HSVC that is represented by Equation (2-2). In this plot, theoretical and simulated results are obtained for variations in the high side voltage reference (VHref) and voltage droop rate (Xdr). These resultant points can be shown to fit each theoretical characteristic very well.

Case B shows the characteristic of reactive current (Iq0) function that is represented by Equation (2-3). In this plot, the theoretical and simulated results are obtained for variations in high side voltage reference (VHref) and reactive current (Iq0). In the case of  $I_q = I_{q0}$ , the high side voltage (VH) is the closer value to the reference (VHref). Therefore, if the reactive current (Iq0) is set to the actual value on the normal operation condition, the high side voltage (VH) can be controlled to the reference (VHref).



Initial Condition :  $P_1 = 0.9 \text{ p.u.}$ ,  $Q_1 = 0.04 \text{ p.u.}$ ,  $V_{Href} = 1 \text{ p.u.}$   
 Step :  $\Delta V_{Href} = 0.01 \text{ p.u.}$ , 100MVA base  
 Points = simulated results, Lines = theoretical characteristics

Figure 2-5. Results for HSVC functions verification

Case C shows the characteristic of the reactive current (Iq0) compensation function by the external reactance (Xe). In this plot, theoretical and simulated results are obtained for variations in high side reference voltage (VHref) with and without this compensation function. These results show that the high side voltage (VH) is controlled near the value of the reference (VHref) both before and after the change of reference, according to the theory presented in this subsection.

Figure 2-6 shows the response characteristics of the advanced HSVC for the data points labeled [2] in Figure 2-5, Case C. The high side voltage (VH) reaches the reference value at about 1.5 sec., is smoothly controlled and stable.

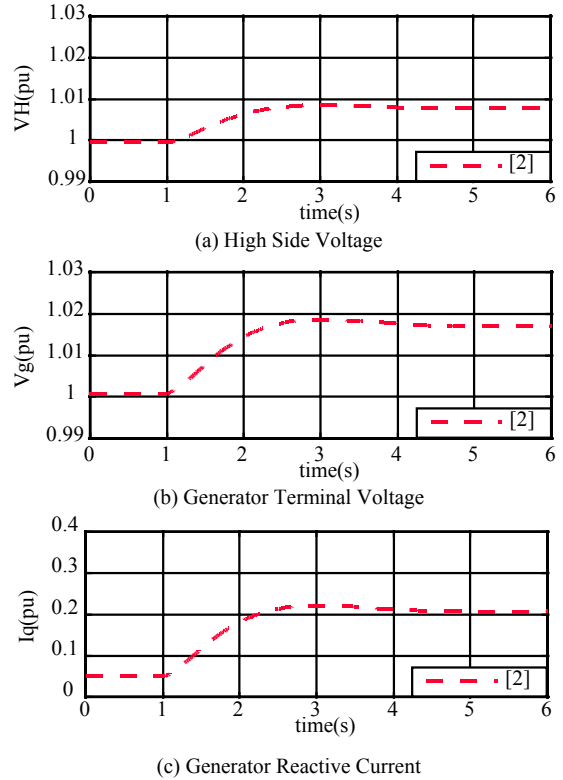


Figure 2-6. Response characteristics of the HSVC shown in Case C, in the points labeled [2] in Figure 2-5

### 2.3 Improvement of Voltage Stability by HSVC

As an example, the improving effect on the voltage stability of a power system by the advanced HSVC was estimated by P-V characteristics [1, 2, 3]. Figure 2-7 shows a model of a simple radial power system with a single machine and load. The resultant P-V characteristics with the application of a static var compensator and the advanced HSVC are respectively shown as Figures 2-8(a) and 2-8(b), and explained in the following paragraphs.

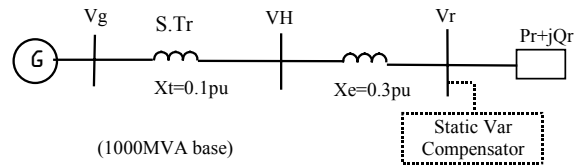
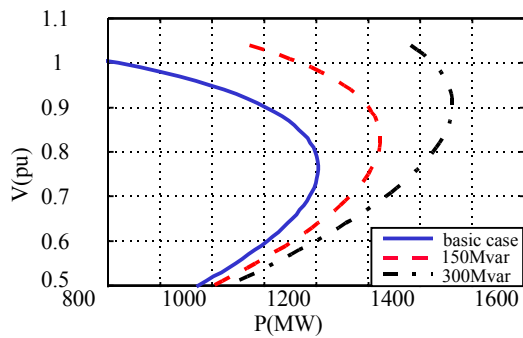
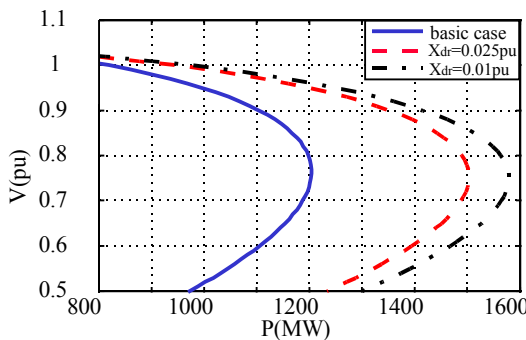


Figure 2-7. Simple model of a single machine and load

For the static var compensator, the allowable sending end power increases with larger capacities of installed static var compensation, but the “nose” voltage tends to go up. This is a common characteristic for shunt compensation that is not necessarily desirable. On the other hand, for the advanced HSVC the allowable sending end power increases with a decrease in the droop rate, thus pushing the nose of the P-V curve out but not up, which is a desirable characteristic of any voltage instability countermeasure. Moreover, since the advanced HSVC can be installed on any generator, including existing facilities, the inherent capability of power plants can be effectively utilized for mitigating voltage instability problems. Therefore, the advanced HSVC is also economically superior as compared to the installation of synchronous condensers, shunt capacitor banks, and FACTS controllers.



(a) P-V curve (static var compensator)



(b) P-V curve (HSVC)

Figure 2-8. P-V characteristics for a simple power system

Reference [5] shows additional analytical development and simulation results illustrating the benefits of HSVC for oscillatory stability, using the well-known de Mello-Concordia model [6]. In addition, Reference [5] also contains discussions with respect to the performance of the HSVC with parallel generator operation.

## 2.4 Installation of HSVC

For new generation plants or for plants undergoing a excitation system controls replacement, the advanced HSVC can be implemented as a software function in a Digital Automatic Voltage Regulator (D-AVR). The D-AVR can also include other functions such as power system stabilizing (PSS), over-excitation limiter (OEL), minimum excitation limiting (MEL), line reactance

drop compensating (LDC), cross current compensating (CCC), volts per hertz limiting (VFL), and/or transient stability over-excitation boosting (TEB).

For existing generation plants, a “self-contained” HSVC function can be added to the existing excitation system controls, in a manner similar to adding a power system stabilizer. Figure 2-9 shows a photo of a Mitsubishi Electric self-contained HSVC unit.



Figure 2-9. Mitsubishi Electric self-contained HSVC unit

## 2.5 Summary on HSVC

This subsection described the advanced High Side Voltage Control (HSVC) regulator, which controls the high side voltage of a generator step-up transformer with no requirement for a direct feedback signal (i.e., measurement) from the high voltage side. The performance of the various functions of advanced HSVC based on a simple power system were introduced in this subsection.

The concept and implementation of the HSVC is an improvement over other methods of supplemental generator excitation control, such as the line drop compensator (LDC) and the power system voltage regulator (PSVR). The advanced HSVC is superior to these methods with respect to control performance, reliability, and economics.

## 3. ADVANCED OVER-EXCITATION LIMITER

### 3.1 Introduction

Mitsubishi Electric has developed an advanced over-excitation limiter (OEL) that not only protects the generator field winding from overheating, but also allows the generator to supply reactive power up to its maximum limitation. This in turn allows for the enhancement of voltage stability of a power system by allowing the full range of reactive power supplying ability of a generator to be utilized. Different from the conventional OEL, the limiting margin of the advanced OEL is estimated from on-line computations based on the field current and voltage measurements of the generator. Hence, the “surplus” and “deficiency” that exists with the conventional OEL margin are omitted in the advanced OEL. In this subsection, the principles and features of the advanced OEL are described and a comparison between the advanced OEL and conventional OEL based on numerical simulations is given.

### 3.2 Principles of Field Winding Protection

Providing a means to allow the full range of reactive power capability of a generator to be utilized is very effective for enhancing the voltage stability of power systems [1, 2, 3]. The reactive power supplying ability of a generator is usually limited as a function of the temperature rise of its field winding. It is standard practice for excitation systems to include an over-excitation limiter function (OEL) to suppress the field current for cases when the temperature of the field winding exceeds an allowable level. According to ANSI Standard (C50-13), the permissible thermal overload of the field winding of round rotor generators is given by the solid curve of Figure 3-1, which assumes that the generator was operating at full rated field current ( $I_{105}$ ) prior to the subsequent increase in field current. This solid curve shows the relationship between the overload current and permissible time delay, and passes through the points shown in Table 3-1.

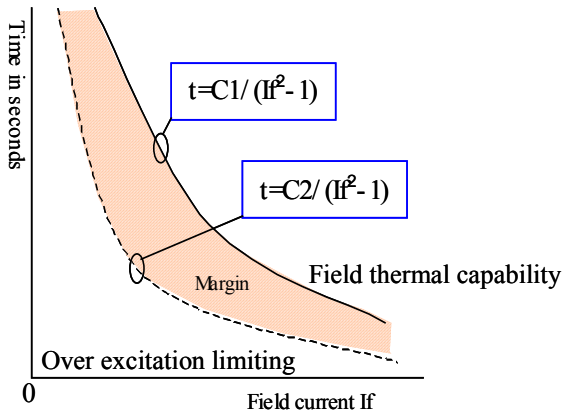


Figure 3-1. Coordination of over-excitation limiting with field winding thermal capability

Table 3-1. Generator Field Capability

Time (seconds)	10	30	60	120
Field voltage/current (Percent of rated)	208	146	125	112

For salient pole generators a separate standard is not directly specified, but standard practice is that the above limits must be satisfied. The solid curve shown in Figure 3-1 can be approximated as:

$$t=C1/(If^2-1) \quad (3-1)$$

where:

t: Time (sec)

If: Field current

C1: Field thermal capability value (more than 30)

Typical over-excitation limiters are more strict than given by Equation (3-1), taking into account the following factors:

- (1) The temperature of the field winding continues to rise from the point where the OEL starts limiting until the field current reverts to its rated value. Hence, a margin corresponding to the temperature rise is necessary.
- (2) If the overload current occurs repeatedly, the initial temperature of the field winding before the OEL operates will be higher than the prescribed value, so a margin corresponding to this “past history” of

overload is also needed.

- (3) A margin is added to account for the time delays existing in the over-excitation detection, operation, etc.

The dotted curve in Figure 3-1 shows the relationship between the overload current and permissible time delay for the actual implementation of the over-excitation limiting function, including all margins. This can also be approximated as:

$$t=C2/(If^2-1) \quad (3-2)$$

where C2 is the limiting value of OEL.

Even the margin between the solid and dotted curves of Figure 3-1 varies depending on the manufacturer and vintage of the generator unit [7]. Over the many possible operating points of a generator, the margin of the conventional OEL can be in “surplus” or “deficiency” of the generator’s actual capability. This is because:

- (1) Although the speed of the field current reduction varies depending on the generator, type of excitation system, and the conditions at the time the OEL is engaged, the margin typically applied is based on the slowest speed of the decreasing field current.
- (2) Even though a margin is added to account for the “past history” of overloading, if the overloading of field current occurs frequently, the added margin may be insufficient. Conversely, if the temperature before the OEL operates is lower than the prescribed initial temperature, then the margin would be too large.

Due to the “surplus” margins as described above, the generator does supply reactive power up to its maximum limitation. This can have a negative impact on power system voltage stability. Therefore, Mitsubishi Electric has developed a new advanced OEL that not only protects the field winding from overheating, but also allows the full capability of the reactive power of a generator to be utilized. This is accomplished by omitting the aforementioned “surplus” and “deficiency” from the margin of the OEL function. The advanced OEL is implemented as a software function in a Digital Automatic Voltage Regulator (D-AVR), as is the high side voltage control (HSVC) function described in Section 2, power system stabilizing (PSS), minimum excitation limiting (MEL), etc.

The advanced OEL has been operating on a synchronous condenser in Japan for a number years [8]. It is playing a critical role for regulating power system reactive power in the system in which it is installed to improve voltage stability, while adequately protecting its field windings.

### 3.3 The Advanced OEL

#### 3.3.1 Operation

Generally, the basic operation of an OEL function can be expressed as:

$$FA+FF+FP+FD \geq C1 \quad (3-3)$$

where:

FA: is the thermal accumulation corresponding to the temperature rise after the field current exceeds the

rated value of  $I_{105}$  ( $I_{105}$  is the field current value when the generator terminal voltage is 1.05 p.u. and the generator output power is 1.0 p.u.);

FF: is the thermal accumulation corresponding to temperature rise when the OEL starts limiting until the field current reverts to its rated value;

FP: is the thermal accumulation corresponding to the initial temperature, taking into account past history;

FD: is the margin for compensating various time delays.

In the conventional OEL, FF, FP, FD are assumed to be uniform values, therefore the operating condition becomes:

$$FA \geq C2 \quad (3-4)$$

where:

$$C2 \geq C1 - FF - FP - FD \quad (3-5)$$

The OEL begins computing when the field current exceeds  $I_{105}$ , and starts to limit the field current when the value of FA becomes larger than C2. Different from the conventional OEL, the new advanced OEL is a computation function (i.e., software) that calculates FF and estimates FP on-line. The structure of the advanced OEL is described next.

### 3.3.2 Structure

The structure of the advanced OEL is shown in Figure 3-2. Field current ( $I_f$ ) and field voltage ( $V_f$ ) measurements are used as the OEL inputs. A computation function is used for calculating FA, FF, and estimating FP. A logical operation function is used to control the operation of the advanced OEL based on the limiting condition of Equation (3-6), and then outputs the limiting signal to the excitation system.

$$FA + FF + FP \geq C1 - FD \quad (3-6)$$

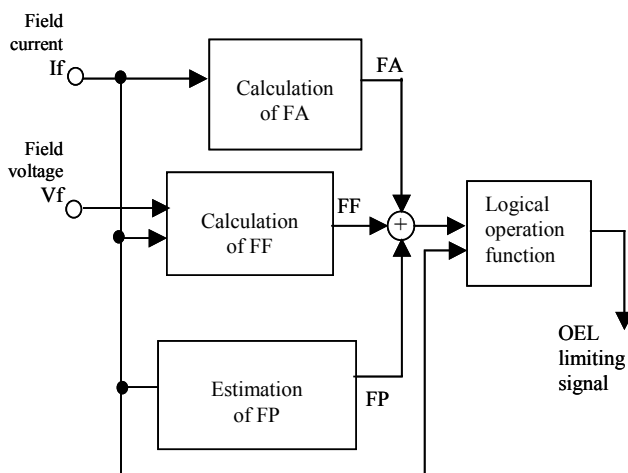


Figure 3-2. Structure of the advanced OEL

### 3.3.3 Thermal Accumulator Calculations

**Thermal Accumulation FA:** The thermal accumulation corresponding to the temperature rise after the field current exceeds  $I_{105}$  is calculated the same as the conventional method, using Equation (3-7).

$$FA = (I_f^2 - 1) t \quad (3-7)$$

**Thermal Accumulation FF:** The operational behavior of an OEL varies depending on the limiting method. Here, the lower signal select circuit is considered. As shown in Figure 3-3, when the OEL starts limiting, the field voltage drops instantly and at the same time, the field current decreases abruptly. Although the time,  $T_r$ , from where the OEL starts limiting until the field current reverts to its rated value can be calculated exactly, it is not practical since a convergence computation is needed to determine  $T_r$ . Here, an alternate approach is adopted to estimate the field current decreasing time,  $T_r$ , according to the inherent crossover frequency  $\omega_c$  of the OEL control loop. Usually, the control target value can be reached within a 1/4 cycle oscillation. Taking into account the time delay for the decreasing field current due to the saturation of the field voltage, and leaving a variation range to the generator field time constant, the field current decreasing time  $T_r$  is estimated as 1/2 cycle of  $\omega_c$  by:

$$T_r = (2\pi / \omega_c) / 2 \quad (3-8)$$

Furthermore, the decreasing characteristic of field current is approximated by the triangle shown in Figure 3-4. Then the thermal accumulation (limiting margin) corresponding to the temperature rise during  $T_r$  can be estimated by:

$$FF = (I_{fmax}^2 - 1) T_r / 2 \quad (3-9)$$

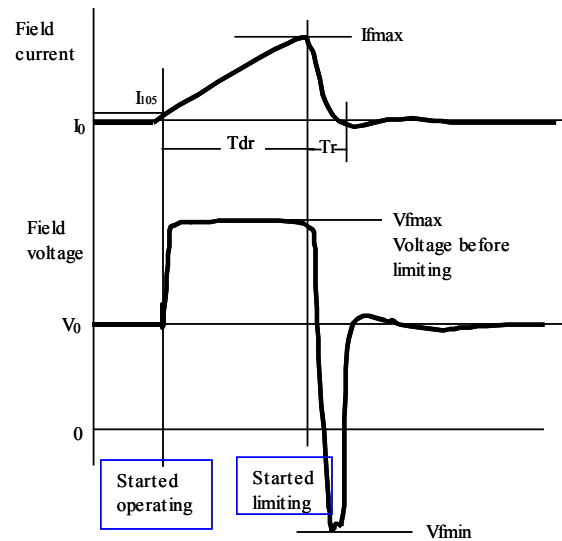


Figure 3-3. Behavior of field voltage and current

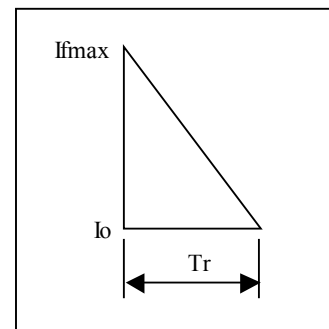


Figure 3-4. Approximated triangle for estimating decreasing field current characteristics

In this way, the surplus can be omitted from the conventional OEL margin corresponding to the temperature rise during  $T_r$ , since the corresponding thermal accumulation is estimated for each generator individually, rather than just leaving an average margin.

**Thermal Accumulation FP:** The thermal accumulation FP corresponding to the initial temperature is:

$$FP = (\theta_a - \theta_0) / C \quad (3-10)$$

where:

- $\theta_a$ : Real temperature of the field winding
- $\theta_0$ : Base temperature of the field winding
- C: Thermal constant

Since the real temperature of field winding is not easy to measure directly, the field winding resistance is used to estimate the real temperature indirectly as shown in Equation (3-12). The resistance of the field winding can be easily calculated by means of the existing output signals of the AVR, (i.e., field current and field voltage) based on the Equation (3-11).

$$R_{fa} = (V_f - V_d) / I_f \quad (3-11)$$

$$\theta_a = R_{fa}(234.5 + \theta_0) / R_{f0} - 234.5 \quad (3-12)$$

where:

- $R_{fa}$ : Resistance of the field winding
- $R_{f0}$ : Base resistant of the field winding
- $V_f$ : Field voltage
- $V_d$ : Slip ring voltage drop

If the real temperature is higher than the prescribed base temperature, the OEL limiting value will be decreased automatically, so that the field winding can be protected from overheating for any repeating or “past history” overload. Conversely, if the real temperature  $\theta_a$  is lower than the base temperature  $\theta_0$ , the OEL limiting value will be increased, thus allowing the generator to provide more reactive power if needed.

### 3.4 Comparison Between Conventional OEL and the Advanced OEL

The purpose of this subsection is to present a comparison of the conventional OEL and the advanced OEL based on numerical simulation, to verify the performance benefits of the advanced OEL.

#### 3.4.1 Simulation Model

The simulation model shown in Figure 3-5 consists of a simplified generator function and an excitation system regulator with an over-excitation limiter function. The simulation condition is to increase the generator terminal voltage reference value ( $V_{tref}$ ) from its rated value to 120% of its rated value.

#### 3.4.2 Using Conventional OEL

The limiting condition of the conventional OEL for a general excitation system is generally set as:

$$FA \geq 5 \quad (3-13)$$

The responses of field voltage,  $V_f$ , and field current,  $I_f$ , and the thermal accumulation, FA, are shown in Figure 3-6. As the plots show, when the field current

exceeds  $I_{105}$ , the OEL starts computing. When the thermal accumulation, FA, exceeds 5, the OEL starts limiting and the field voltage and current revert to their rated values.

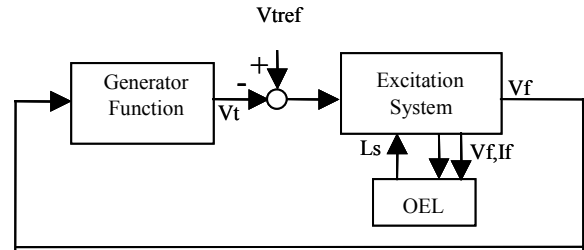


Figure 3-5. Simulation model ( $V_t$  is the generator voltage,  $V_{tref}$  is the reference voltage,  $V_f$  and  $I_f$  are the field voltage and current, and  $L_s$  is the limiting signal)

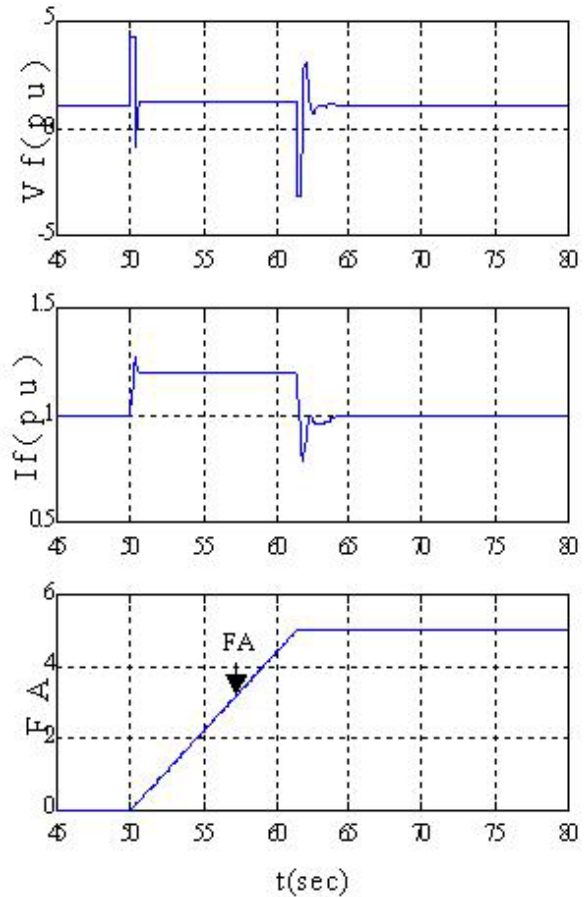


Figure 3-6. Results by conventional OEL

#### 3.4.3 Using Advanced OEL

As described in Section 3.2, the limiting condition of the advance OEL is:

$$FA + FF + FP \geq C1 - FD$$

According to ANSI Standard (C50-13), the value of C1 is over 30. Assuming the delay margin FD is smaller than 5, the limiting condition is set as:

$$FA + FF + FP \geq 25 \quad (3-14)$$

The value FP is calculated on-line based on the field voltage and current measurements in the actual implementation of the advanced OEL. The temperature deviation (i.e., past history) is also considered here, thus, in the simulations, FP is taken to be the following fixed values:

**Case 1:** If the real temperature before the advanced OEL starts operating equals the specified base temperature, then  $FP=0.0$ .

**Case 2:** If the overload current occurred frequently, the real temperature before the advanced OEL starts operating would be higher than the specified base temperature, then  $FP=23$ .

**Case 3:** If the real temperature before the advanced OEL starts operating is lower than the specified base temperature, then  $FP= -10$ .

The responses of field voltage,  $V_f$ , and field current,  $I_f$ , and the thermal accumulations  $FA$ ,  $FF$  and  $FP$ , in each case are shown in Figure 3-7 (Case 1), Figure 3-8 (Case 2) and Figure 3-9 (Case 3). As the results show, when the field current exceeds  $I_{105}$ , the OEL starts computing, similar to the conventional OEL. Then when the sum of the thermal accumulations exceeded 25, the advanced OEL starts limiting, and the field voltage and current revert to their rated values.

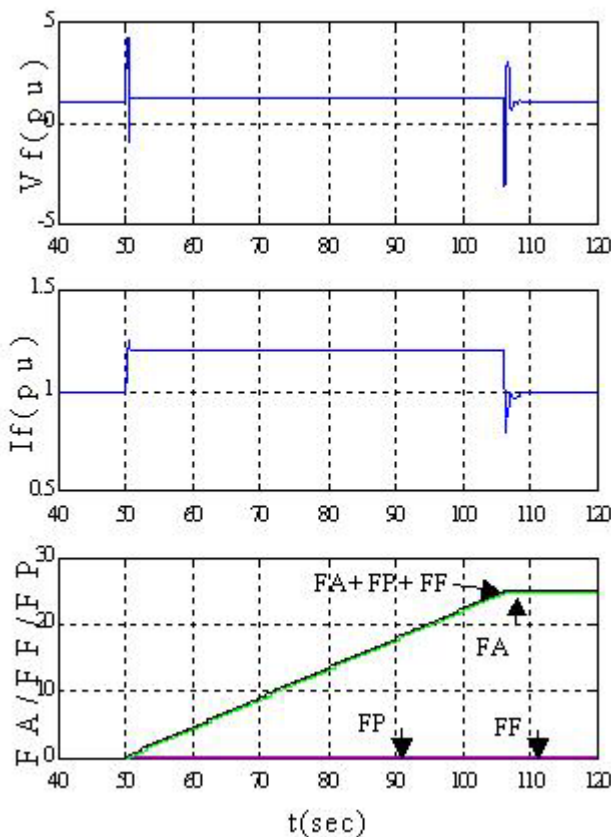


Figure 3-7. Results of Case 1 (real temperature before the advanced OEL starts operating equals the specified base temperature)

### 3.4.4 Comparison of Results

The results for comparison are listed in Table 3-2. The values of  $FF$  are very small since a high response excitation system is used in this simulation model. However, the estimated value of  $FF$  is very close to the real difference value  $\Delta FA$ , where  $FA1$  is the value when the OEL started limiting,  $FA2$  is the value when the field current reverted to its rated value, and  $\Delta FA$  is the difference of  $FA2$  and  $FA1$ . Therefore, this confirms that the estimation of  $FF$  is appropriate.

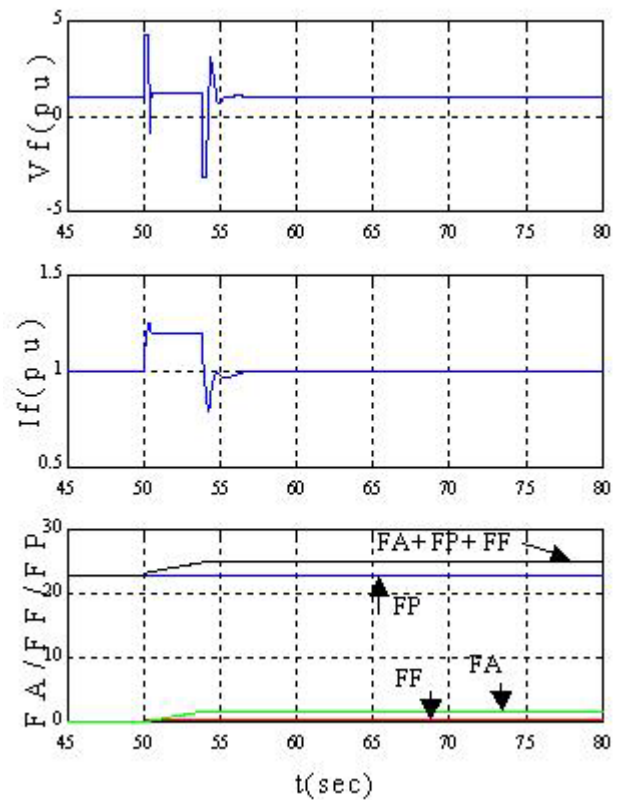


Figure 3-8. Results of Case 2 (real temperature before the advanced OEL starts operating is higher than the specified base temperature to account for recent past overloads)

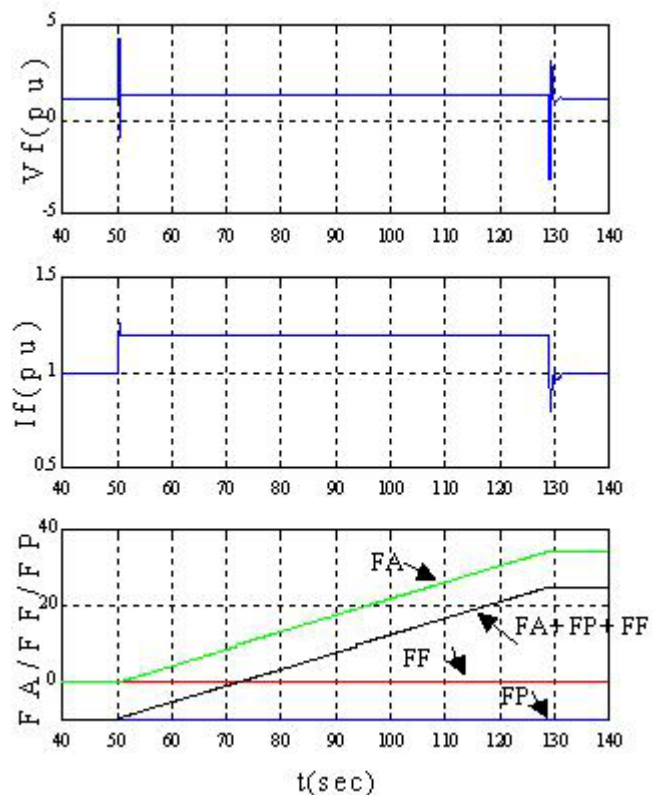


Figure 3-9. Results of Case 3 (real temperature before the advanced OEL starts operating is lower than the specified base temperature)

**Table 3-2. A Comparison of Conventional (C-OEL) and Advanced (A-OEL) Over-Excitation Limiters**

CASE	FA1	FA2	ΔFA	FF	FP	Tdr
C-OEL	5.00	-	-	-	-	11.7
Case 1 (A-OEL)	24.65	25.04	0.39	0.52	0.00	56.8
Case 2 (A-OEL)	1.65	2.05	0.40	0.52	23.0	3.8
Case 3 (A-OEL)	34.65	35.04	0.39	0.52	-10.0	78.8

The time values for Tdr (the time when the OEL starts until the limiting begins) are very different depending on the value of FP. In other words, the limiting margin can be regulated automatically according to the initial temperature by using the advanced OEL. In the case of FP=0 (real temperature before the OEL starts operating equals the specified base temperature) and FP= -10 (real temperature before the OEL starts operating is lower than the specified base temperature), the time Tdr is extended to 56.8 and 78.8 seconds. This is much longer than the time using the conventional OEL (11.7 seconds). This means that the generator can provide more reactive power if needed, during this extended time. FP=23 (real temperature before the OEL starts operating is higher than the specified base temperature to account for recent past overloads) is for an extreme case where the initial temperature is very high. Here, if the conventional OEL is used in this case, the limiter would start at 11.7 sec after the overload current occurred. With the advanced OEL, the limiter would start within 3.8 seconds hence, the generator winding can be protected more securely.

### 3.5 Summary on the Advanced OEL

This section introduced a new advanced over-excitation limiter (OEL) developed by Mitsubishi Electric. The advanced OEL is a software function in a Digital Automatic Voltage Regulator (D-AVR). The D-AVR can also include other functions such as power system stabilizing (PSS), high side voltage control (HSVC), minimum excitation limiting (MEL), line reactance drop compensating (LDC), cross current compensating (CCC), volts per hertz limiting (VFL), and/or transient stability over-excitation boosting (TEB).

The advanced OEL performs an on-line calculation of the thermal accumulations corresponding to the temperature rise during the period where the OEL starts limiting until the field current reverts to its rated value, and additionally estimates the thermal accumulation corresponding to the initial temperature before the OEL operates. Hence, any “surplus” and “deficiency” contained in the margins of the conventional OEL are omitted from the advanced OEL. Therefore, the advanced OEL is able to contribute to the improvement of power system voltage stability by enhancing the reactive power supplying ability of generators, as well as protecting the generator field winding from overheating.

Reference [8] shows an application of a 100 Mvar synchronous condenser that has operated for a number of years in Japan with the advanced OEL.

## 4. ADJUSTABLE SPEED MACHINE

### 4.1 Introduction

This subsection proposes an active power control method to prevent voltage instability and severe voltage dips by compensating the power system load. This active power control is applied to an adjustable speed machine (ASM), which can be implemented by a doubly-fed machine that utilizes an ac field excitation system rather than dc field excitation. The ASM in the simulation example described in this subsection is primarily used as a synchronous condenser, but includes a flywheel for short-term active power injection into the system. Since an ASM has a high response, it is able to supply both reactive power and active power rapidly, as required by the power system.

### 4.2 Principles of Adjustable Speed Machines

#### 4.2.1 Operation and Construction

Constant speed synchronous machines are the primary source of electricity generated in power systems. Normally, a constant speed generator is excited by a dc field excitation system on fixed poles on the rotor. Thus the frequency of the generated voltage/current is a function of the rotor speed and number of poles.

The use of doubly-fed machines for large-scale generation have become practical through advances in power electronics and control technology [10, 11]. In contrast to a constant speed machine, an adjustable speed generator (or motor) is excited by an ac field. The rotor poles are not fixed and can be rotated forward or backward by changing the phase-sequence and frequency of the excitation current. The rotor may rotate backward or forward with respect to the poles, either adding to or subtracting from the synchronous frequency of the stator flux [12]. The frequency of the generated voltage/current is a function of the sum of the rotor speed and the frequency of the ac excitation:

$$n_s = n_r \pm n_2 \quad (4-1)$$

where:

$n_s$  is the frequency on the stator

$n_r$  is the rotational speed of the rotor

$n_2$  is the frequency of the ac excitation

In synchronous operation (i.e. steady-state), the frequency of the rotor field equals the frequency of the stator, and is set by the system (e.g., 50 or 60 Hz). Since the rotational speed of the field of an ASM can be changed by adjusting the frequency of the ac excitation, the active power can be controlled rapidly by increasing or decreasing the rotational speed, according to the relationship:

$$P = M (d\omega/dt) \quad (4-2)$$

From this relationship, it can be observed that an ASM can rapidly control the active power based on the energy stored in its rotor inertia. The ASM allows for energy to be stored or withdrawn while the stator frequency remains constant. The basic concept of an ASM is illustrated in Figure 4-1. The doubly-fed machine typically utilizes a cylindrical rotor with three-

phase distributed field windings. The rotor is excited with an ac field, which is supplied by a three-phase converter (either cycloconverter or voltage-sourced converter).

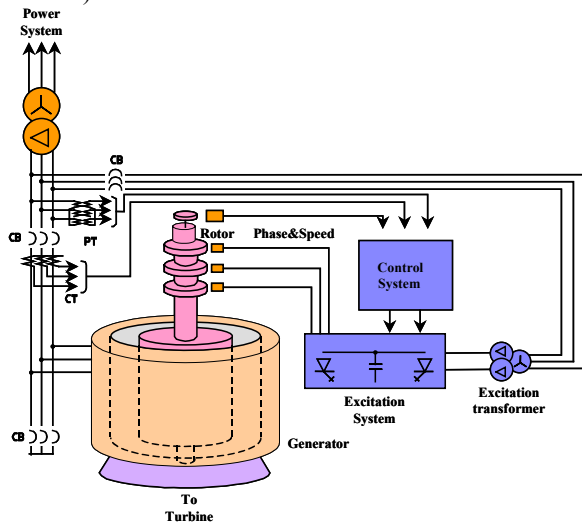


Figure 4-1. Concept of an adjustable speed machine

#### 4.2.2 Active Power Control Using an Adjustable Speed Machine to Improve Stability

Generally, countermeasures to improve voltage stability primarily relate to reactive power compensation or voltage control [1-6, 8]. Active power control has only recently been considered. This is in part due to the fact that active power control response of synchronous generators is too slow to be beneficial for short-term voltage instability mitigation. However, by means of the ASM, active power control for preventing voltage instability can be realized. The following items summarize the main advantages of ASMs [9, 10]:

**Adjustable Speed:** An ASM is excited by its AC excitation system, which is its rotor. Hence, the value of the rotor speed is determined by the frequency difference between the power system and the excitation system. It is possible to control the rotor speed of the ASM to a desired value according to the system operation requirements by regulating the frequency of the excitation system.

**Condenser Ability:** An ASM can be used as a synchronous condenser to supply reactive power. However, unlike a conventional synchronous condenser, the ASM condenser can transform its rotational energy into active power. Hence, with a flywheel with sufficient storage capacity, the ASM condenser is able to provide active power on a short-term basis.

**P-Q Independent Control:** By means of the d-q axis individual excitation method, the active power P and reactive power Q of an ASM can be controlled independently.

**High Response of Power Control:** Making use of the rotational energy of the ASM, an extremely high response is possible (at least 300 times higher than a synchronous generator), thus active power control can be realized by the excitation system.

**High Impact on Rotor-Angle Stability:** The transient stability and oscillatory stability of an ASM system are excellent, since the angle of the ASM can be controlled directly. Constant speed machines can

withstand internal angle transient changes of not more than 60 to 90 degrees while remaining stable. In contrast, an ASM generator with a speed range of +/- 15% during a 4 second ramping interval could develop an internal rotor angle change of 7200 degrees [12], thus, providing orders of magnitude more benefit for transient and oscillatory stability.

**High Impact on Long-Term and Short-Term Voltage Stability:** An ASM operated as a synchronous condenser contributes to long-term voltage stability because it extends transmission system limitations by way of compensating reactive power and improving voltage control. Additionally, by taking advantage of its high power control response, the ASM condenser or generator can also contribute to short-term voltage stability using its stored energy in the rotor inertia.

As an illustration of the application, Figure 4-2 shows an ASM located between the sending-end and receiving-end of a power system. In steady-state operation, the ASM compensates reactive power according to the system requirements and suppresses voltage fluctuations. A voltage dip detecting function can be added to the active power control system of the ASM. Thus, once an abrupt voltage drop or frequency drop is detected, the ASM rapidly outputs active power to compensate the deficiency in active power supplied to the load, until the system recovers. The output value of the active power is determined according to the voltage drop level and frequency variation level. The maximum output electrical energy of the ASM is determined by the capacity of its rotor inertia.

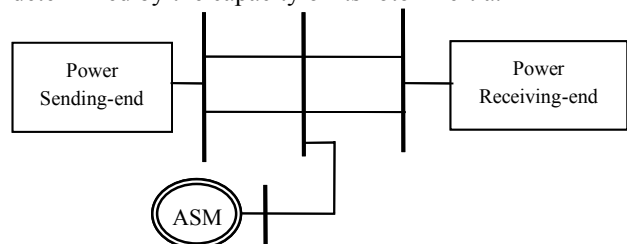


Figure 4-2. Illustration of an ASM condenser application

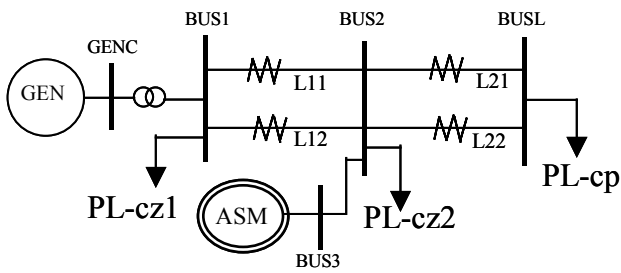
### 4.3 System Simulation Example for an ASM Condenser

#### 4.3.1 System Model

As an application example, the ASM with the proposed active power control function is used in a single synchronous generator and hybrid load power system, as shown in Figure 4-3. Here, the synchronous generator supplies two constant impedance loads and one constant power load through four transmission lines. Here, the ASM is a condenser and is located at a bus at the midpoint of the transmission system.

The synchronous generator is equipped with an automatic voltage regulator (AVR). The ASM condenser is equipped with a voltage control system, a reactive power control system, and an active power control system with a voltage dip detecting function. The data for the synchronous generator and the ASM are listed in Reference [9].

To identify the effectiveness of the active power control using an ASM condenser for preventing short-term voltage instability, a numerical simulation was performed, as described in the next subsection.



- GEN: Synchronous generator (1000MVA)
- PL-cp: Constant power load (600MW)
- PL-cz1: Constant impedance load (200MW)
- PL-cz2: Constant impedance load (200MW)
- ASM: ASM condenser (400MVA)

Figure 4-3. Simulation model

### 4.3.2 Simulation of Transmission Line Tripping

The simulation condition considered is for a case where the system transfer impedance increases. Here, the transmission line L12 is tripped at  $t=1.17$ sec and re-closed at  $t=2.17$ sec (see Figure 4-3). To distinguish the effect of active power control for preventing voltage instability from the basic voltage control, the simulations with and without the voltage dip detecting function of the ASM were performed separately.

With the ASM active power control voltage dip detecting function not active, the voltage drops abruptly after line L12 is tripped, and then the system collapses since there is insufficient active power supplied to the constant power load. For this case, the total impedance of the transmission lines is extended to 0.25 p.u. The simulation results are shown in Figure 4-4.

Adding the voltage dip detecting function to the active power control of the ASM condenser, the voltage collapse is avoided (even when the total impedance of the transmission lines is extended to 0.47 p.u.) The simulation results are shown in Figure 4-5. After line L12 tripped, the ASM outputs active power instantly to compensate for the lost power from the sending-end by reducing its rotational speed. Hence, the voltage dip recovers sooner as well. After the line L12 is re-closed, the system returns to its original operating state and the active power of the ASM condenser is reduced to zero within 1 sec.

Reference [9] also contains a simulation example for a major disturbance caused by a large sudden change in load dispatch, illustrating further benefits of the ASM condenser for improving short-term voltage stability.

### 4.4 Summary on Adjustable Speed Machines

In this subsection, an active power control method for preventing short-term voltage instability was proposed. This active power control was applied to an adjustable speed machine, which can be implemented by a doubly-fed machine that utilizes ac field excitation system rather than dc excitation.

As an application example, an ASM with the proposed active power control function was used with a single synchronous generator and hybrid load power system. The ASM described in the example was primarily used as a synchronous condenser and included

a flywheel for short-term active power injection into the system. This ASM condenser can support the power system to avoid voltage collapse or excessive voltage dips by compensating both active and reactive power supply to the system immediately after a disturbance. One scenario was examined, namely a transmission line tripping, with and without the proposed active power control function. The simulation results showed that the power system survived from voltage collapse after the disturbances for the case where the active power control function was in-place. Therefore, the effectiveness of the active power control by means of an ASM condenser for preventing short-term voltage instability was identified.

The ASM technology discussed in this subsection focused on the application to a synchronous condenser rather than a generator for the application at a midpoint of a transmission system. In situations where an adjustable speed generator can be applied, the effect of improving voltage stability will be more dramatic than with the adjustable speed condenser shown here.

## 5. SUMMARY AND CONCLUSIONS

Voltage instability problems are attracting increasing attention in today's power systems, with wide-ranging emphasis on power system operation, planning, and control. These problems are becoming a more serious concern with the ever-increasing utilization and higher loading of existing transmission systems, particularly with increasing energy demands, and competitive generation and supply requirements. It is well established that enhancing the reactive power supplying ability of a power system is an effective means to improve voltage stability. However, other means are available for the improvement of voltage stability that can be applied on generators by enhancing their reactive and active power control and voltage control. This paper described three such methods, summarized as follows:

**High Side Voltage Control (HSVC):** The HSVC regulator controls the high side voltage of a generator step-up transformer with no requirement for a direct feedback signal (i.e., measurement) from the high voltage side. The concept and implementation of the HSVC is an improvement over other methods of supplemental generator excitation control, such as the line drop compensator (LDC) and the power system voltage regulator (PSVR). The advanced HSVC is superior to these methods with respect to control performance, reliability, and economics.

**Over-Excitation Limiter (OEL):** A new advanced over-excitation limiter (OEL) developed by Mitsubishi Electric was introduced. The advanced OEL performs an on-line calculation of the thermal accumulations corresponding to the temperature rise during the period where the OEL starts limiting until the field current reverts to its rated value, and additionally estimates the thermal accumulation corresponding to the initial temperature before the OEL operates. Hence, any "surplus" and "deficiency" contained in the margins of the conventional OEL are omitted from the advanced OEL. Therefore, the advanced OEL is able to contribute to the improvement of power system voltage

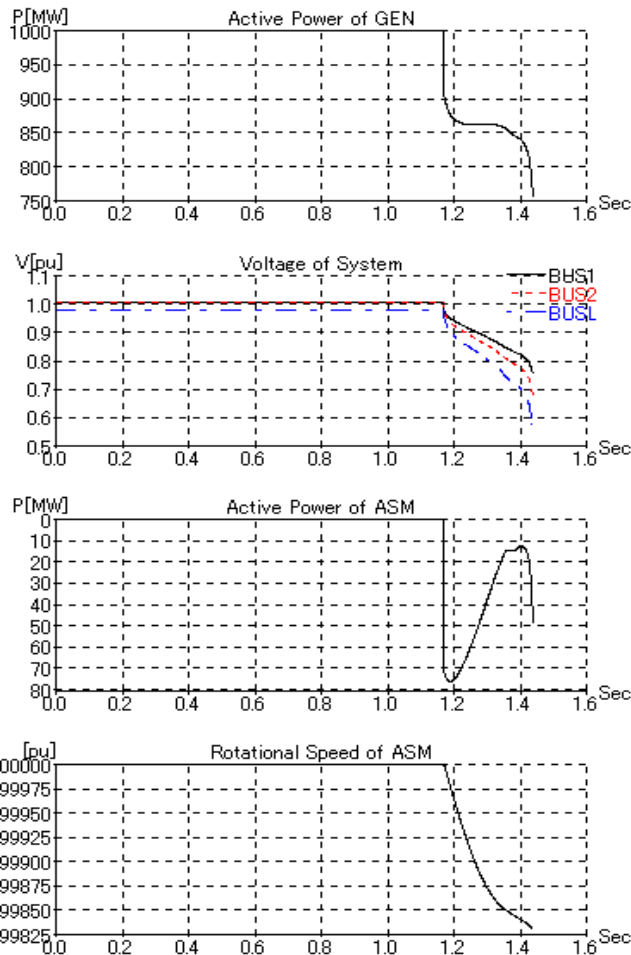


Figure 4-4. System responses after 1 line tripped (without voltage dip detecting function)

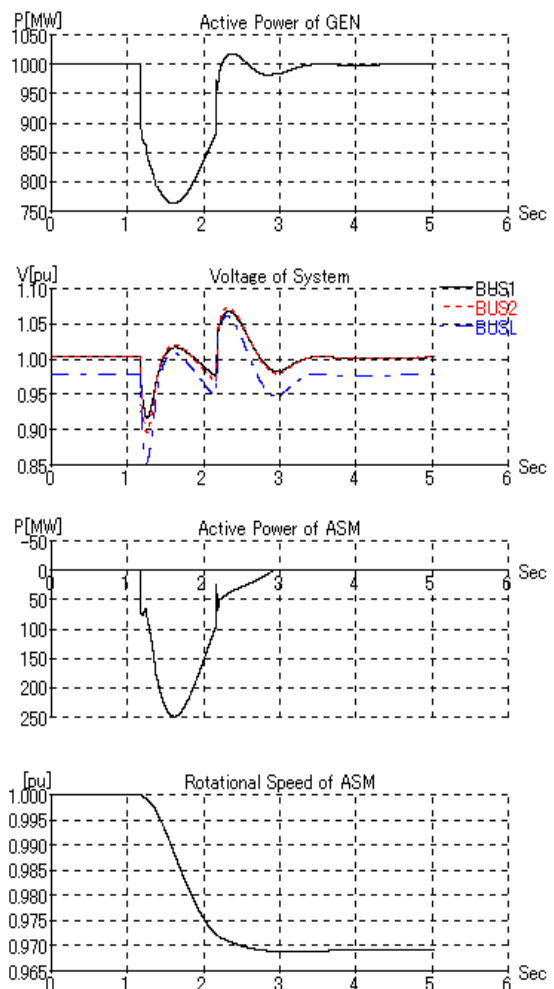


Figure 4-5. System responses after 1 line tripped (with voltage dip detecting function)

stability by enhancing the reactive power supplying ability of generator, as well as protecting the generator field winding from overheating.

**Adjustable Speed Machine (ASM):** An active power control method for preventing short-term voltage instability was proposed. This active power control was applied to an ASM, which can be implemented by a doubly-fed machine that utilizes an ac field excitation system rather than dc excitation. The ASM described in this subsection is primarily used as a synchronous condenser, and includes a flywheel for short-term active power injection into the system. This ASM can support the power system to avoid voltage collapse or excessive voltage dips by compensating both active and reactive power supply to the system immediately after a disturbance.

## REFERENCES

- [1] C.W. Taylor, Power System Voltage Stability, McGraw-Hill, Inc., 1994.
- [2] P. Kundur, Power System Stability and Control, McGraw-Hill, Inc., 1994.
- [3] T. Van Cutsem, C. Vournas, Voltage Stability of Electric Power Systems, Kluwer Academic Publishers, 1998.

- [4] T. Michigami, N. Onizuka, S. Kitamura, "Development of Advanced Generator Excitation Control Regulator (PSVR) for Improving Voltage Stability of a Bulk Power Transmission System," The Institute of Electrical Engineers of Japan, Vol. 110-B, No. 11, November 1990, pp. 887-894.
- [5] H. Kitamura, M. Shimomura, J. Paserba, "Improvement of Voltage Stability by the Advanced High Side Voltage Control Regulator," Proceedings of the 2000 IEEE PES Summer Meeting, Seattle, WA, July 2000, pg. 278-283.
- [6] F.P. de Mello and C. Concordia, "Concepts of Synchronous Machine Stability as Affected by Excitation Control," IEEE Transactions on Power Apparatus and Systems, Vol. PAS-88, Apr. 1969, pp. 316-329.
- [7] C.R. Mummert, "Excitation System Limiter Models for Use in System Stability Studies," Proceedings of the 1999 PES Winter Meeting, New York, NY, pp. 187-192.
- [8] M. Shimomura, Y. Xia, M. Wakabayashi, J. Paserba, "A New Advanced Over Excitation Limiter for Enhancing the Voltage Stability of Power Systems," Proceedings of the 2001 IEEE PES Winter Power Meeting, Columbus, OH, January/February 2001.

[9] Y. Xia, M. Shimomura, J. Paserba, "An Active Power Control for Preventing Instability Using an Adjustable Speed Machine," Proceedings of the IEEE PES for the 2001 Summer Power Meeting, Vancouver, British Columbia, July 2001.

[10] S.C. Verma, et al. "A Comparative Study of Dynamic Performance of an Adjustable Speed Generator-Motor based Frequency Converter and HVDC Frequency Converters," Proceedings of the 2000 CEPSI at Manila Philippines, pp. 173-180, October, 2000.

[11] S. Furuya, S. Fujiki, T. Hioki, T. Yanagisawa, S. Okazaki, S. Kobayashi, "Development and Achieved Commercial Operation Experience of the World's First Commissioned Converter-Fed Variable-Speed Generator-Motor for a Pumped Storage Plant," *CIGRE Paper 11-104*, Paris, August 1992.

[12] J.J. Paserba, C. Concordia, E. Lerch, D.P. Lysheim, D. Ostojic, B.H. Thorvoldsson, J.E. Dagle, D.J. Trudnowski, J.F. Hauer, N. Janssens, "Opportunities for Damping Oscillations by Applying Power Electronics in Electric Power Systems," *CIGRE Symposium on Power Electronics in Electrical Power Systems*, Tokyo, Japan, May 1995.

#### BIOGRAPHIES

**John J. Paserba, Donald J. Shoup, and Robert T. Hellested** are employed by Mitsubishi Electric Power Products Inc. (MEPPI), Power Systems Division, Energy Systems Department, based in Warrendale, Pennsylvania.

**Masaru Shimomura and Seiichi Tanaka** are employed by Mitsubishi Electric Corporation (MELCO), Energy and Industrial Systems Center, Power Plant and Systems Department based in Kobe, Japan.